Int. J. Heat Mass Transfer. Vol. 28, No. 1, pp. 219–233, 1985
Printed in Great Britain

0017–9310/85 $3.00 + 0.00

The toroidal thermosyphon with known heat flux

MIHIR SEN,*† EDUARDO RAMOS† and CÉSAR TREVIÑO*

*Departamento de Fluidos y Térmica, Div. de Ingeniería Mecánica y Eléctrica, Facultad de Ingeniería, U.N.A.M., 04510 México D.F., México; † Departamento de Energía Solar, Instituto de Investigaciones en Materiales, U.N.A.M., 04510 México D.F., México

(*Received* 11 *July* 1983 *and in revised form* 15 *May* 1984)

Abstract—This paper discusses the behavior of a toroidal thermosyphon with known heat flux around the loop. Criteria are first established for steady state solutions. The transient governing equations are then transformed to an infinite set of ordinary differential equations. The flow velocity, however, can be determined from a set of three equations which decouple from the rest. The existence and stability of the critical points of these equations are examined, and typical numerical solutions for different values of the governing parameters are presented. Chaotic solutions are shown to be possible.

1. INTRODUCTION

FREE convection loops have been studied in reference to naturally occurring phenomena as well as for engineering applications. Examples include the study of solar heating systems, nuclear reactor cooling, geological flows, etc.

One-dimensional thermosyphon models can be developed for a closed loop of perfectly general form [1, 2]. There are some advantages in this formulation but the principal disadvantage lies in the complexity of the governing equations which inhibits analytical treatment. The time-dependent problem has to be treated, for the present, through the study of specific cases.

The literature on the subject shows that different configurations have been studied, but no mathematical (or other) advantage has been put forward for any of them. By and large, importance has been placed on the rectangular [3–5] and toroidal loops [6–14].

Most studies on the toroidal loop have considered one of the following modes of heating:

(a) Known heating flux over part of the loop and convective cooling with constant heat transfer coefficient and known wall temperature over the rest.

(b) Known heating flux over the whole loop.

(c) Convective heat transfer with constant coefficient and known wall temperature over the whole loop.

Other treatments have included consideration of the temperature change in the cooling heat exchanger or property variations [9–11, 15].

Generally speaking, experimental work has approximated heating mode (a). Creveling *et al.* [6] were the first to observe instability in single-phase flow. Damerell and Schoenhals [7] reported the results of experiments carried out on an asymmetrically heated toroidal loop. Their theoretical analysis, though approximate, was the first to recognize the multiplicity of time-independent solutions to the thermosyphon problem with heating modes (a) and (b). (Similar results given in [16] are for a slightly different case.) They could not observe experimentally the existence of these multiple solutions. Greif *et al.* [8] confirmed numerically the instability which had been pointed out by Creveling *et al.* [6]. Other results on the toroidal thermosyphon have been reported in [9–11], all using numerical methods.

The time-dependent problem will be studied by a Galerkin-type technique which was first introduced by Saltzman [17] in 1962 to enable him to transform the problem of natural convection in a fluid layer to an equivalent infinite set of ordinary differential equations. To facilitate analysis, these were later truncated to a set of three by Lorenz [18], who obtained and studied the equations which now bear his name. The first application of this method to the toroidal thermosyphon problem was made in 1972 in a brief but excellent paper by Malkus [19]. The convective heating was from a constant wall temperature, while the known heating flux was restricted to the cosine modes only in the Fourier expansion. These assumptions permit decoupling of the first three equations, which are the Lorenz equations, from the rest. The same method can be applied and the Lorenz equations obtained for heating mode (c) [13]. The double diffusive problem is discussed in [12].

A recent paper by Hart [20] tackles a general heating flux, including heating mode (a), under certain symmetry conditions. His assumption of symmetry, not only in the heating flux but also in the temperature field, permitted him to decouple three "master" equations from the rest. These three which can be transformed into the Lorenz equations describe the dynamical problem entirely. The basic assumption of temperature symmetry is, however, difficult to justify since numerical calculations [8] show distinct asymmetry about a vertical diameter even if the heating is symmetrical.

In the Appendix we analyze a specific case of heating mode (a) in which no temperature symmetry is assumed. The infinite set of ordinary differential equations so obtained remains coupled. Therefore, any

NOMENCLATURE

a,b	non-dimensional heat flux parameters defined in Section 4
c	specific heat of fluid
D	diameter of thermosyphon tube
g	acceleration due to gravity
$\tilde{g}$	local gravitational acceleration
L	length of loop
q	heat influx per unit length
Q	non-dimensional heat influx
R	mean radius of torus
s	longitudinal coordinate
T	temperature
ΔT	characteristic temperature difference
t	time
u	mean fluid velocity
v	non-dimensional fluid velocity
x,y,z	variables defined in Section 4
x'	root mean square value of $x(\tau)$.

Greek symbols

β	coefficient of thermal expansion
θ	angular coordinate
ν	kinematic viscosity of fluid
ρ	fluid density
σ	radian frequency
τ	non-dimensional time
τ^*	time period
$\Delta\tau$	step length for numerical integration
ϕ	non-dimensional fluid temperature.

Subscripts and superscripts

c	cosine coefficient of Fourier series
s	sine coefficient of Fourier series
$\bar{}$	time independent solution
$\hat{}$	amplitude of perturbations.

truncation to a finite set would involve an approximation similar to that made by Lorenz [18]. The general heat transfer case is discussed in [21].

In the present work we consider a toroidal thermosyphon with heating mode (b). Even though it is difficult to achieve experimentally, this condition also permits an exact reduction of the problem to a set of three ordinary differential equations, without the need for any symmetry assumption. The resulting equations, furthermore, have some of the characteristics of the Lorenz equations, including chaotic solutions.

2. TOROIDAL THERMOSYPHON

For a general loop configuration, momentum and energy considerations lead to [1, 4]

$$\frac{\mathrm{d}u}{\mathrm{d}t}+\frac{32\nu}{D^2}u=\frac{\beta}{L}\int_0^L T(s,t)\tilde{g}(s)\,\mathrm{d}s \tag{1}$$

$$\frac{\pi\rho cD^2}{4}\left(\frac{\partial T}{\partial t}+u\frac{\partial T}{\partial s}\right)=q(s) \tag{2}$$

where the dependent variables are $u(t)$ and $T(s,t)$, being the mean velocity and temperature, respectively. The local component of the gravitational acceleration along the negative s direction along the loop is denoted by $\tilde{g}(s)$. For simplicity, frictional force corresponding to fully developed flow in a straight pipe of circular cross-section is considered, even though other power law friction factors can be easily considered [20]. All fluid properties are taken constant except for the density which varies linearly with temperature in the buoyancy term. Viscous dissipation and axial conduction which have been considered in [14] and [22], respectively, are neglected here.

For any thermosyphon loop, all functions of the longitudinal coordinate s, like $\tilde{g}(s)$, $T(s,t)$ and $q(s)$ are L-periodic in s. Especially, for the gravity function we can use a Fourier series expansion of the form

$$\tilde{g}(s)=\sum_{n=1}^{\infty}\{g_n^{\mathrm{c}}\cos(2\pi ns/L)+g_n^{\mathrm{s}}\sin(2\pi ns/L)\}. \tag{3}$$

The "simplest" problem would result in taking g_1^{c} and g_1^{s} different from zero and $g_n^{\mathrm{c}}=g_n^{\mathrm{s}}=0$ for $n>1$. We have then

$$\begin{aligned}\tilde{g}(s)&=g_1^{\mathrm{c}}\cos(2\pi s/L)+g_1^{\mathrm{s}}\sin(2\pi s/L)\\&=g\cos(2\pi s/L-\theta_0)\end{aligned} \tag{4}$$

where $g^2=(g_1^{\mathrm{c}})^2+(g_1^{\mathrm{s}})^2$ and $\theta_0=\tan^{-1}(g_1^{\mathrm{s}}/g_1^{\mathrm{c}})$, g being the acceleration due to gravity. This gravity function corresponds to a toroidal thermosyphon. Choosing the origin of s correctly, we can make θ_0 zero without any loss of generality. It is customary to use the angular coordinate θ given by $\theta=s/R$, where R is the mean radius of the torus. Measuring θ from the horizontal (Fig. 1) we have

$$\tilde{g}(\theta)=g\cos\theta. \tag{5}$$

The governing equations (1) and (2) reduce to

$$\frac{\mathrm{d}u}{\mathrm{d}t}+\frac{32\nu}{D^2}u=\frac{\beta g}{2\pi}\int_0^{2\pi}T\cos\theta\,\mathrm{d}\theta \tag{6}$$

and

$$\frac{\pi\rho cD^2}{4}\left(\frac{\partial T}{\partial t}+\frac{u}{R}\frac{\partial T}{\partial\theta}\right)=q(\theta). \tag{7}$$

These equations can be non-dimensionalized by using

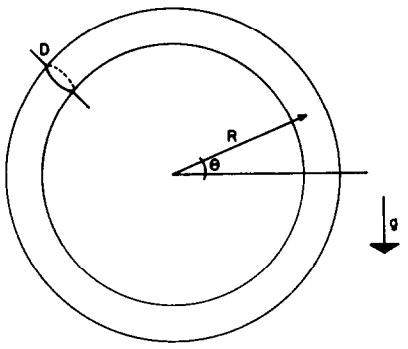

FIG. 1. Toroidal thermosyphon.

the variables

$$\tau = 32\nu t/D^2$$

$$v(\tau) = uD^2/32\nu R$$

$$\phi(\theta,\tau) = (T-T_0)/\Delta T$$

$$Q(\theta) = q(\theta)/(8\pi\rho c\Delta T\nu)$$

where T_0 is a reference temperature and

$$\Delta T = 2048\pi R\nu^2/\beta g D^4.$$

Equations (6) and (7) then take the form

$$\frac{dv}{d\tau} + v = \int_0^{2\pi} \phi \cos\theta \, d\theta \tag{8}$$

$$\frac{\partial\phi}{\partial\tau} + v\frac{\partial\phi}{\partial\theta} = Q(\theta). \tag{9}$$

3. TIME-INDEPENDENT SOLUTIONS

Indicating the time-independent values of $v(\tau)$ and $\phi(\theta,\tau)$ by $\bar{v}$ and $\bar{\phi}(\theta)$, respectively, equations (8) and (9) simplify to

$$\bar{v} = \int_0^{2\pi} \bar{\phi} \cos\theta \, d\theta \tag{10}$$

and

$$\bar{v}\frac{d\bar{\phi}}{d\theta} = Q(\theta). \tag{11}$$

Integrating equation (11) around the loop, we get

$$\int_0^{2\pi} Q(\theta)\, d\theta = 0 \tag{12}$$

which is a necessary, but not sufficient, condition for the existence of the following time-independent solutions:

$$\bar{\phi}(\theta) = \frac{1}{\bar{v}}\int_0^{\theta} Q(\theta')\, d\theta' + \bar{\phi}_0 \tag{13}$$

$$\bar{v} = \pm\sqrt{\left\{\int_0^{2\pi} \cos\theta\left[\int_0^{\theta} Q(\theta')\, d\theta'\right] d\theta\right\}} \tag{14}$$

where $\bar{\phi}_0$ is a constant.

Multiplicity of solutions due to the $\pm$ sign in equation (14) was first pointed out by Damerell and Schoenhals [7]. For the existence of these solutions we must add to (12) the following restriction obtained from (14):

$$\int_0^{2\pi} \cos\theta\left[\int_0^{\theta} Q(\theta')\, d\theta'\right] d\theta \geqslant 0. \tag{15}$$

Since $Q(\theta)$ is a 2π-periodic function in θ, we can write

$$Q(\theta) = \sum_{n=1}^{\infty} (Q_n^c \cos n\theta + Q_n^s \sin n\theta). \tag{16}$$

The time-independent velocity (14) is

$$\bar{v} = \pm\sqrt{(-Q_1^s\pi)} \tag{17}$$

and the condition (15) becomes

$$Q_1^s \leqslant 0. \tag{18}$$

The coefficient Q_1^s of the Fourier series expansion of the heat flux function $Q(\theta)$ plays an important role in the existence of a steady velocity within the thermosyphon. Physically, of course, all that condition (18) means is that we must heat below and cool on top in order to obtain flow at a constant velocity. The stability of this solution is a different matter which will be dealt with later.

4. TIME-DEPENDENT PROBLEM

Analytic solutions for equations (8) and (9) have not been obtained. Following Malkus [19], we can reduce them to an infinite set of ordinary differential equations using the 2π-periodicity of the non-dimensional temperature $\phi(\theta,\tau)$ in the coordinate θ. We write

$$\phi(\theta,\tau) = \phi_0^c(\tau) + \sum_{n=1}^{\infty} [\phi_n^c(\tau)\cos n\theta + \phi_n^s(\tau)\sin n\theta]. \tag{19}$$

Substituting this and equation (16) into (8) and (9), we have

$$\frac{dv}{d\tau} + v = \pi\phi_1^c(\tau) \tag{20}$$

$$\frac{d\phi_0^c}{d\tau} + \sum_{n=1}^{\infty}\left(\frac{d\phi_n^c}{d\tau}\cos n\theta + \frac{d\phi_n^s}{d\tau}\sin n\theta\right) + v\sum_{n=1}^{\infty}(-n\phi_n^c \sin n\theta + n\phi_n^s \cos n\theta) = \sum_{n=1}^{\infty}\{Q_n^c \cos n\theta + Q_n^s \sin n\theta\}. \tag{21}$$

Multiplying equation (21) by $\cos m\theta$ and integrating from 0 to 2π we get

$$\frac{d\phi_m^c}{d\tau} + vm\phi_m^s = Q_m^c, \quad m = 0,1,2,\ldots \tag{22}$$

where $Q_0^c = 0$.

Repeating the process with $\sin m\theta$,

$$\frac{d\phi_m^s}{d\tau} - vm\phi_m^c = Q_m^s, \quad m = 1,2,\ldots \tag{23}$$

Equations (20), (22) and (23) represent an infinite set of ordinary differential equations in the unknowns $v(\tau)$, $\phi_0^c(\tau)$, $\phi_m^c(\tau)$, $\phi_m^s(\tau)$, $(m = 1, 2, \ldots)$. The velocity $v(\tau)$ is uniquely determined, however, by a subset of three equations which decouple from the rest. For $m = 1$, equations (22) and (23) become

$$\frac{d\phi_1^c}{d\tau} + v\phi_1^s = Q_1^c \tag{24}$$

$$\frac{d\phi_1^s}{d\tau} - v\phi_1^c = Q_1^s. \tag{25}$$

The unknowns are the non-dimensional velocity $v(\tau)$ and the Fourier coefficients ϕ_1^c and ϕ_1^s of the non-dimensional temperature distribution. A three-dimensional phase space can be used to plot the trajectory of the solution in time.

The equations can be put in a neater form by writing $v = x$, $\pi\phi_1^c = y$, $\pi\phi_1^s = z$, $\pi Q_1^c = a$, $-\pi Q_1^s = b$. With this notation, equations (20), (24) and (25) take the form

$$dx/d\tau = y - x \tag{26}$$

$$dy/d\tau = a - zx \tag{27}$$

$$dz/d\tau = xy - b. \tag{28}$$

The rest of the equations (22) and (23) can be explicitly integrated once $v(\tau)$ is known.

The physical significance of parameters a and b can be clarified in the following manner. Consider a heating flux of the form

$$Q = -\frac{\hat{Q}}{\pi} \sin(\theta - \alpha) \tag{29}$$

which represents heating and cooling sections inclined with respect to the horizontal. From (16) we obtain

$$Q_1^c = +\frac{\hat{Q}}{\pi} \sin\alpha$$

$$Q_1^s = -\frac{\hat{Q}}{\pi} \cos\alpha$$

with $Q_n^c = Q_n^s = 0$ for $n > 1$.

The parameters a and b can be obtained as

$$a = \hat{Q} \sin\alpha$$

$$b = \hat{Q} \cos\alpha.$$

On keeping $\hat{Q}$ constant and varying α, the point (b, a) on a map such as Fig. 2 would trace a circle with its center at the origin and radius $\hat{Q}$.

The important case of symmetrical heating and cooling about a vertical diameter of the torus corresponds to $a = 0$.

5. CRITICAL POINTS AND THEIR LINEAR STABILITY

For $b < 0$, equations (26)–(28) do not have any critical points. At $b = 0$ there is a limit point bifurcation and two critical points P^+ and P^- appear for $b > 0$.

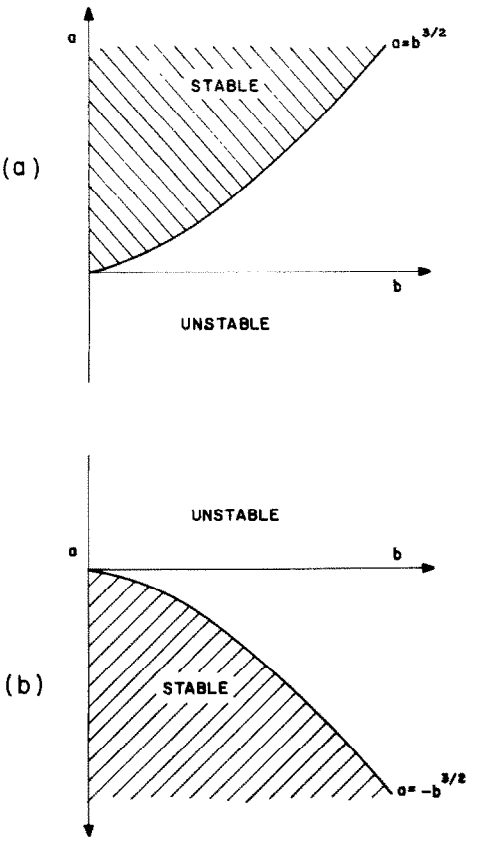

FIG. 2. Stability map for (a) P^+ and (b) P^-.

These are given by the coordinates

$$(\bar{x}, \bar{y}, \bar{z}) = \pm(\sqrt{b}, \sqrt{b}, a/\sqrt{b}). \tag{30}$$

The positive sign is for P^+ and the negative sign for P^-. These results check with the time-independent solutions obtained in Section 3.

Linear stability of the critical points can be analyzed by putting

$$x = \bar{x} + \hat{x} \exp(\sigma\tau) \tag{31}$$

$$y = \bar{y} + \hat{y} \exp(\sigma\tau) \tag{32}$$

$$z = \bar{z} + \hat{z} \exp(\sigma\tau) \tag{33}$$

where the amplitudes $\hat{x}$, $\hat{y}$ and $\hat{z}$ of the perturbations are small. Substituting in equations (26)–(28) and linearizing, we get

$$\begin{bmatrix} \sigma+1 & -1 & 0 \\ \bar{z} & \sigma & \bar{x} \\ \bar{y} & \bar{x} & -\sigma \end{bmatrix} \begin{bmatrix} \hat{x} \\ \hat{y} \\ \hat{z} \end{bmatrix} = \begin{bmatrix} 0 \\ 0 \\ 0 \end{bmatrix}. \tag{34}$$

Solutions for $\hat{x}$, $\hat{y}$ and $\hat{z}$, are non-trivial only if the determinant of the equations vanishes.

This reduces to the characteristic equation

$$\sigma^3 + \sigma^2 + (\bar{x}^2 + \bar{z})\sigma + \bar{x}(\bar{x} + \bar{y}) = 0. \tag{35}$$

Substituting the coordinates of the critical points (30),

we have

$$\sigma^3+\sigma^2+(b\pm a/\sqrt{b})\sigma+2b=0. \quad (36)$$

The positive sign is for the critical point P^+ and the negative for P^-. For stability the roots should have negative real parts. Applying the Routh–Hurwitz criterion (see, for example, [23]), we can obtain stability maps for each of the critical points P^+ and P^-, as shown in Fig. 2.

6. NUMERICAL TRANSIENT SOLUTIONS

The divergence of the right hand side of equations (26)–(28) is -1. This means that the system is dissipative and any initial volume in the x, y, z phase space will be reduced in time at a rate proportional to $e^{-\tau}$. Some kind of attractor is expected for every bounded solution.

Results based on a Runge–Kutta numerical scheme have been obtained using a time step-length $\Delta\tau = 0.01$. These fall into the following representative cases:

(a) $b < 0$, no critical point exists. The fluid velocity x goes to zero while one or both Fourier coefficients of the temperature y and z become unbounded. This case corresponds to heating at a higher level than the cooling. Of course, since heat conduction rather than convection is the dominant heat transfer mode here, the present mathematical model does not represent reality.

(b) $b > 0, a > b^{3/2}$, two critical points exist, one (P^+) stable and the other (P^-) unstable. Starting from any initial condition different from P^-, the time-dependent solution is attracted to the critical point P^+ as time goes on. Figure 3 shows the projections of such a solution on the xy and xz plane as well as the function $x(\tau)$, for the initial condition $x(0) = y(0) = z(0) = 1$ with $a = 2$, $b = 1$.

(c) $b > 0, a = b^{3/2}$, two critical points exist, one (P^+) neutrally stable and the other (P^-) unstable. Near P^+ the characteristic equation (36) can be factorized for $a = b^{3/2}$ to give the roots $-1, \pm\sqrt{(2b)}$i. Near this critical point then, the negative root leads to a damped solution while the conjugate imaginary roots correspond to oscillations at a frequency $\sqrt{(2b)}$. Passing from the stable to the unstable side of the neutral curve, we change from damped to stationary oscillations. This represents a Hopf bifurcation. Figure 4 illustrates the neutrally stable case with $a = b = 1$ and $x(0) = 2$, $y(0) = 1$ and $z(0) = 1$.

(d) $b > 0$, $a < b^{3/2}$, two critical points exist, both unstable. For values of a near $b^{3/2}$, the neutrally stable limit cycle solutions in the previous case carry over as illustrated in Fig. 5 with $a = 0.75$, $b = 1$ and $x(0) = y(0) = z(0) = 1$. Farther away from the neutral stability curve, this periodic motion becomes gradually more complex as shown in Fig. 6 for $a = 0.5$, $b = 1$ and $x(0) = y(0) = z(0) = 1$. In fact, for $a = 0.25$, $b = 1$ and $a = 0$, $b = 1$ (Figs 7 and 8, respectively), the trajectories of the solution in three-dimensional phase space take on very complicated shapes. Plotted against time, the dependent variables appear chaotic as in strange attractor solutions [24]. At any sufficiently large time, the calculated value of the variables are very sensitive to small changes in initial conditions.

7. PERIODIC SOLUTIONS

For periodic solutions it can be shown that, for one-dimensional thermosyphons of any configuration, the

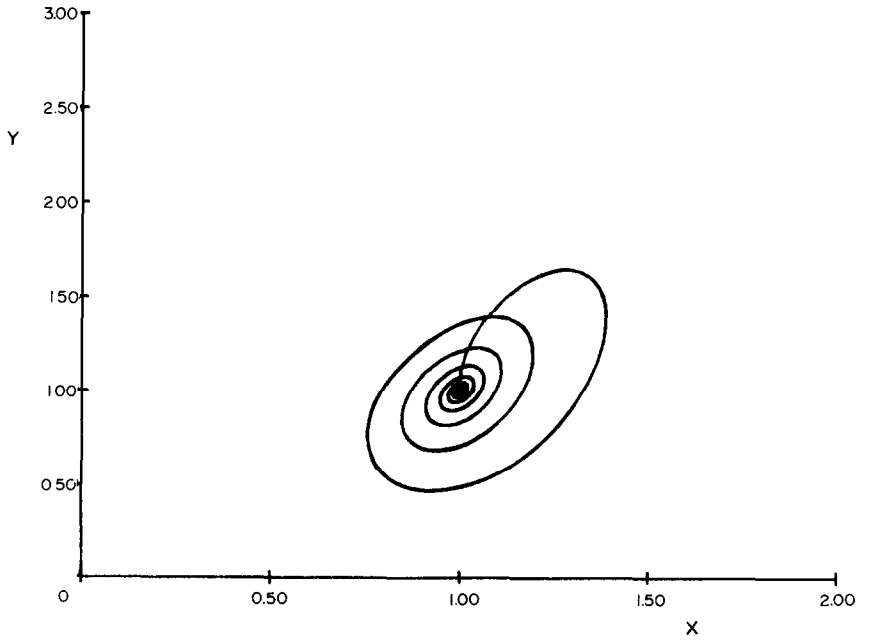

FIG. 3. (a)

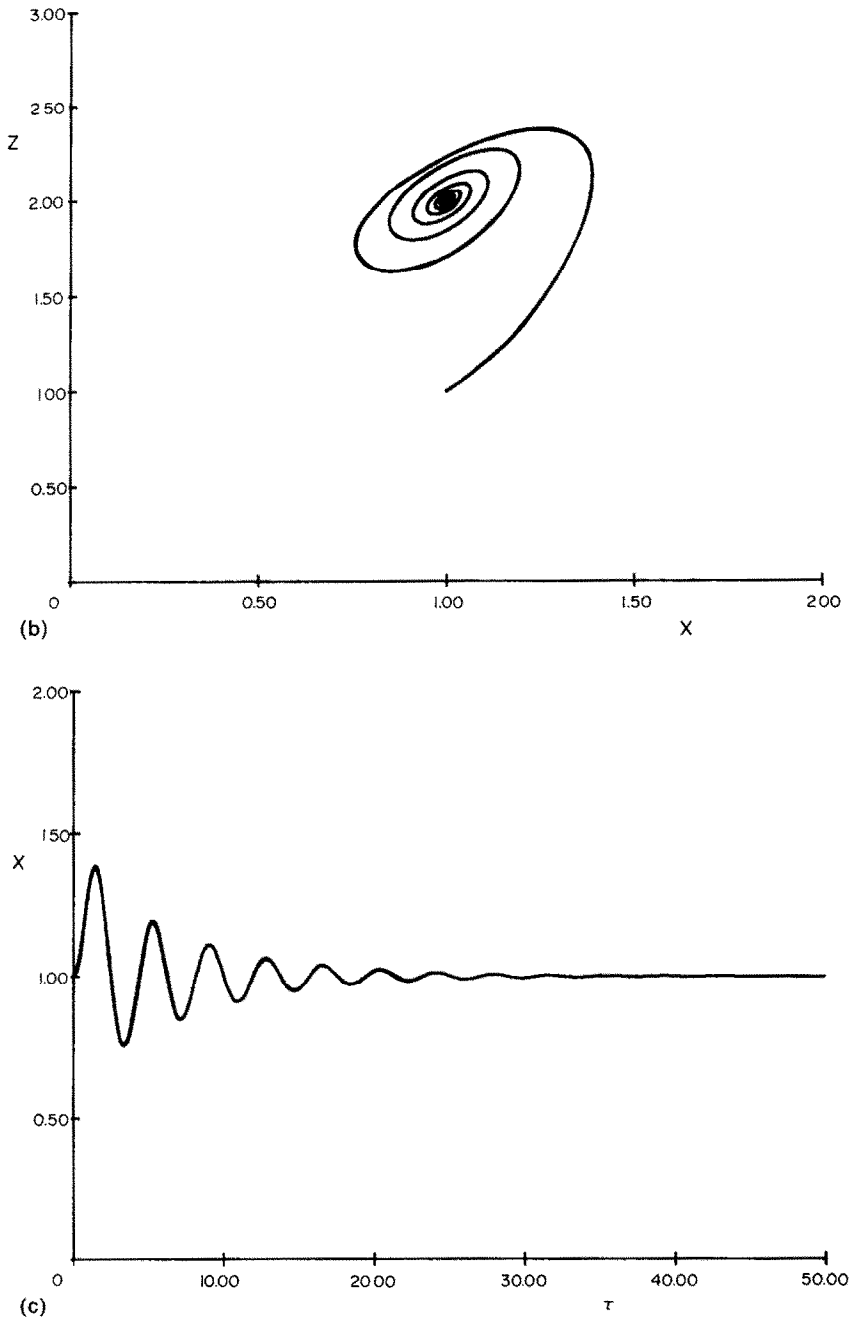

FIG. 3. Numerical solution for $a = 2$, $b = 1$. Initial conditions (1, 1, 1). (a) xy projection, (b) xz projection, and (c) $x(\tau)$.

root mean square velocity is equivalent to the value calculated for the (possible unstable) steady state velocity [1]. The present is only a special case and the theorem can be demonstrated very simply. We assume x, y and z in equations (26)–(28) to be periodic such that

$$\begin{aligned} x(\tau_0) &= x(\tau_0+\tau^*) \\ y(\tau_0) &= y(\tau_0+\tau^*) \\ z(\tau_0) &= z(\tau_0+\tau^*) \end{aligned} \tag{37}$$

for all τ_0.

We indicate an average over a period τ^* by

$$\langle\cdot\rangle = \frac{1}{\tau^*}\int_{\tau_0}^{\tau_0+\tau^*} \cdot \, d\tau. \tag{38}$$

Multiplying equation (26) by x and averaging over a period we get

$$\langle x^2\rangle = \langle xy\rangle. \tag{39}$$

Averaging equation (28) we have

$$\langle xy\rangle = b. \tag{40}$$

From these and the time-independent solutions (30),

$$x'/\bar{x} = 1 \tag{41}$$

where x' is the root mean square value of the periodic solution, defined by $\sqrt{(\langle x^2 \rangle)}$.

In the stable region of the parameters a and b, we know that $x \to \bar{x}$ as $\tau \to \infty$. The time-independent solution $x = \bar{x}$ satisfies the conditions (37), not only for all τ_0 but also for all τ^*. The root mean square velocity x' is the constant velocity $\bar{x}$ itself and equation (41) is thus satisfied as $\tau \to \infty$.

In the unstable region, the solution ranges from periodic to apparently chaotic. Even here, the root mean square values x' tend to $\bar{x}$ for large integration times. This is demonstrated in Table 1 in which $x'/\bar{x}$ is shown for $a = 0$ and different values of b. τ_0 and τ^* are taken as zero and 1000, respectively. Since relation (41) is closely satisfied, it would seem that even in this chaotic region, the solution can be taken to be periodic with a sufficiently long period.

In the experimental results reported by Creveling *et al.* [6], values of the "time-averaged" mass flux

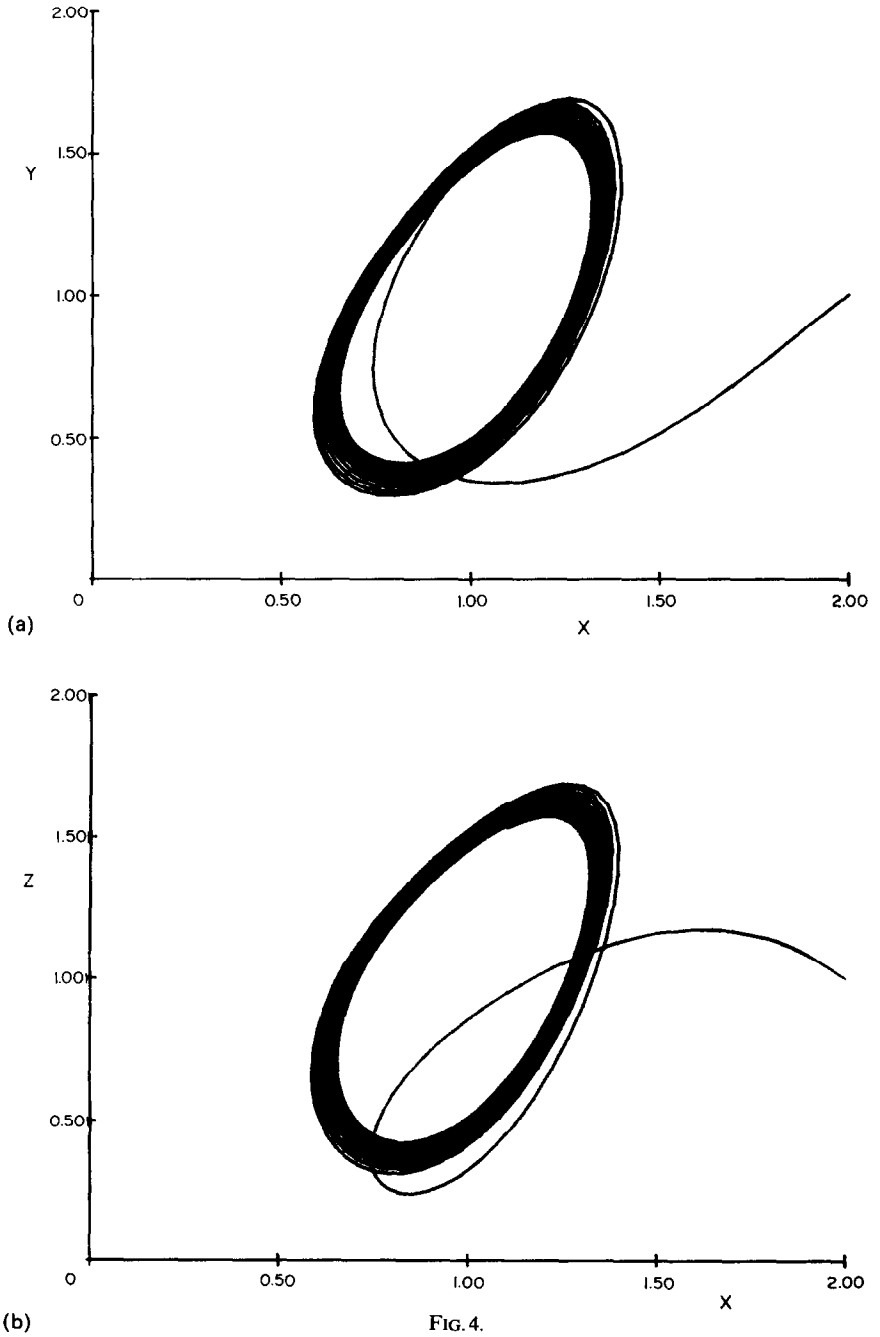

FIG. 4.

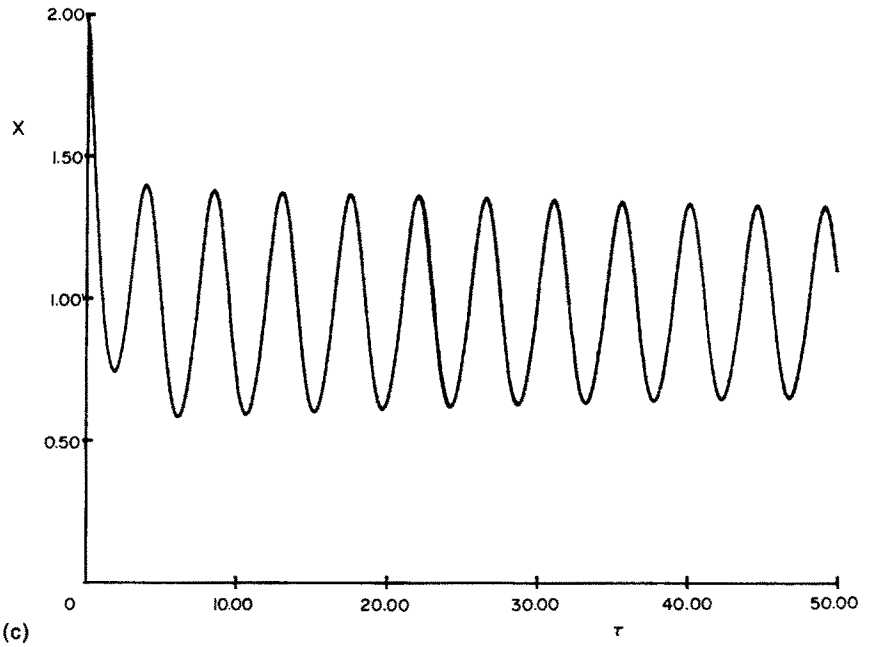

FIG. 4. Numerical solution for $a = 1$, $b = 1$. Initial conditions (2, 1, 1). (a) xy projection, (b) xz projection, and (c) $x(\tau)$.

corresponded to calculated steady state values. In their words "it is clear that the correlation between the steady-state prediction and experiment is suitable not only for steady flows, but for the unstable oscillatory flow conditions as well".

8. CONCLUSIONS AND DISCUSSION

The toroidal configuration is the simplest thermosyphon loop that can be considered for theoretical study. The present work has assumed a known heat

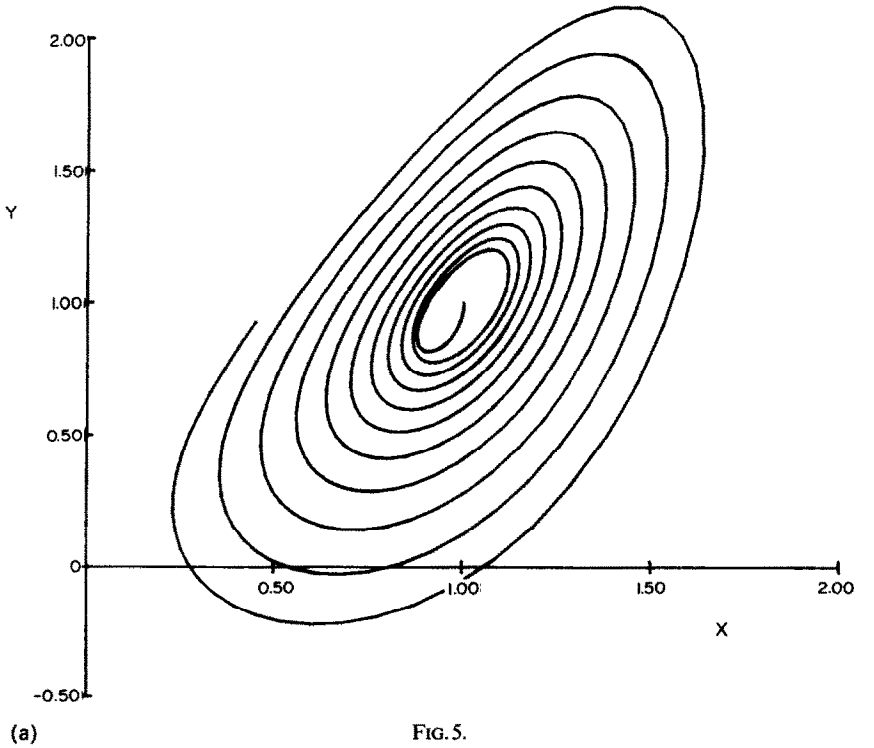

FIG. 5.

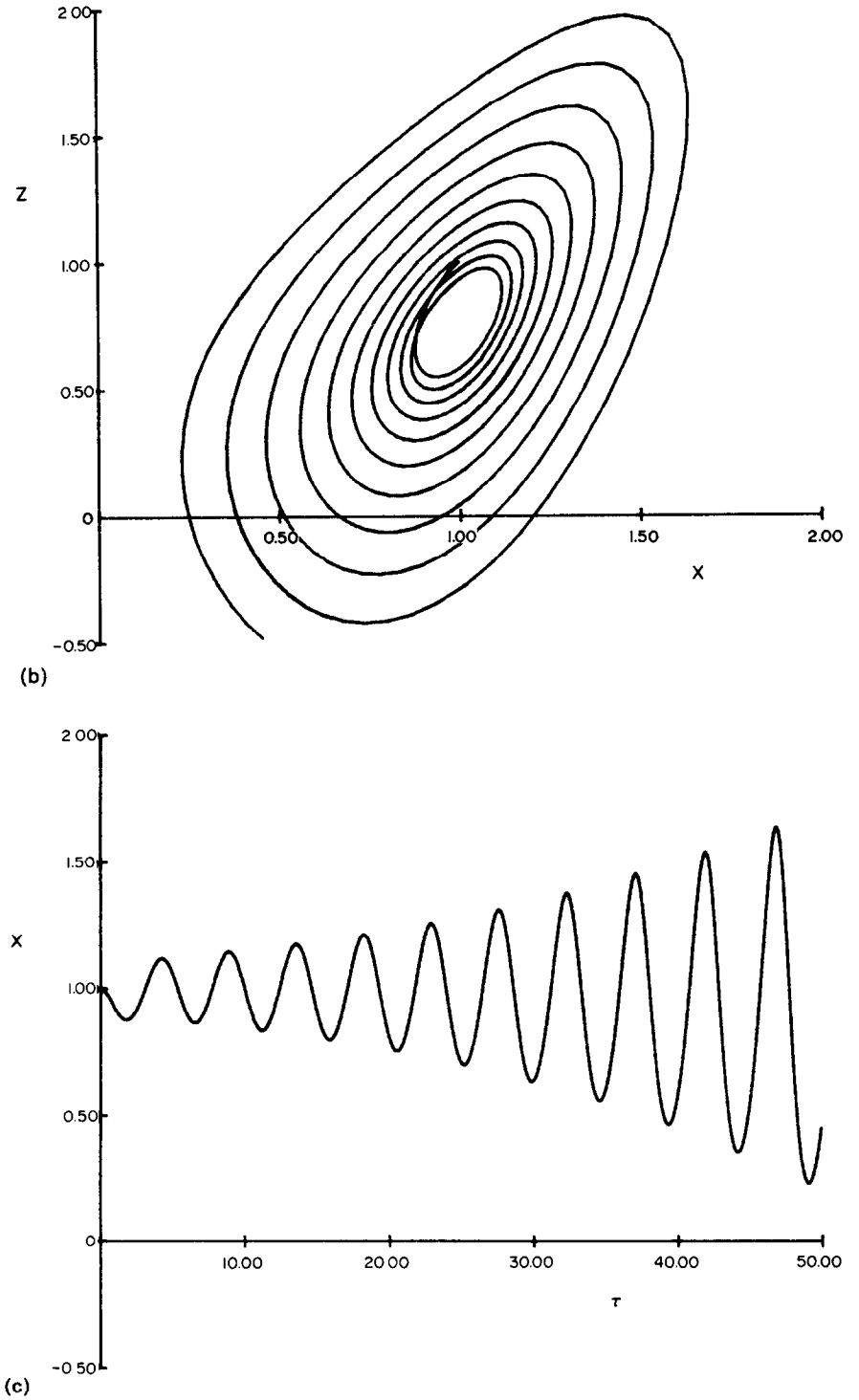

FIG. 5. Numerical solution for $a = 0.75, b = 1$. Initial conditions (1, 1, 1). (a) xy projection, (b) xz projection, and (c) $x(\tau)$.

flux distribution all around the torus. The complete transient problem is shown to depend on the solution of three non-linear ordinary differential equations (26)–(28). A wide range of solutions to those equations are possible. Depending on the heating distribution, we can obtain constant stable, periodic or apparently chaotic behaviors. For all these cases we get the same root mean square fluid velocity as for time-independent flow under the same conditions. All these results have qualitative confirmation in reported experiments, though no quantitative comparison is possible.

The equations governing the toroidal thermosyphon

with heating mode (c) can be reduced to a different set of three non-linear ordinary differential equations [12, 13]. These are in the notation of [13]

$$dx/d\tau = p(y-x)$$

$$dy/d\tau = -y+rx-zx+r'$$

$$dz/d\tau = xy-z.$$

On taking $r' = 0$, corresponding to symmetric heating about a vertical diameter, these equations reduce to the Lorenz equations [18] which have been amply studied. For $r < 1$, only one critical point exists at the origin and is stable. In the range $1 < r < p(p+4)/(p-2)$, two other stable critical points appear and the critical point at the origin is unstable. If $r > p(p+4)/(p-2)$ all critical points are unstable and chaotic

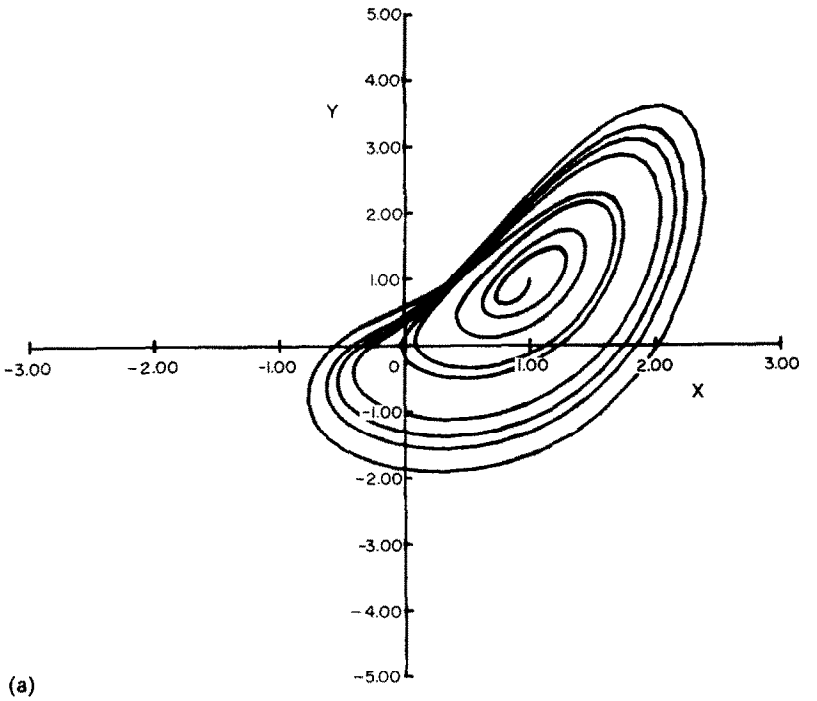

(a)

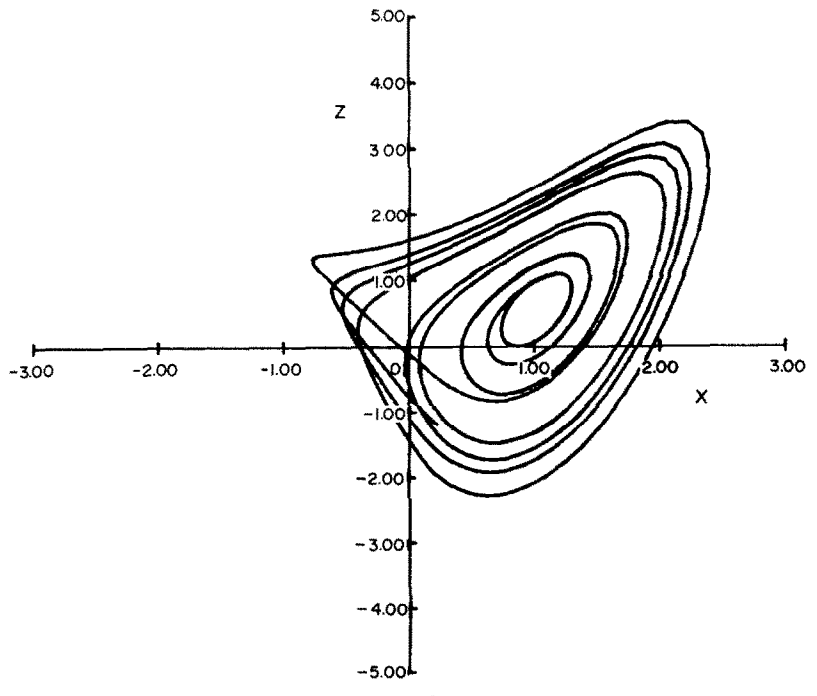

(b)

FIG. 6.

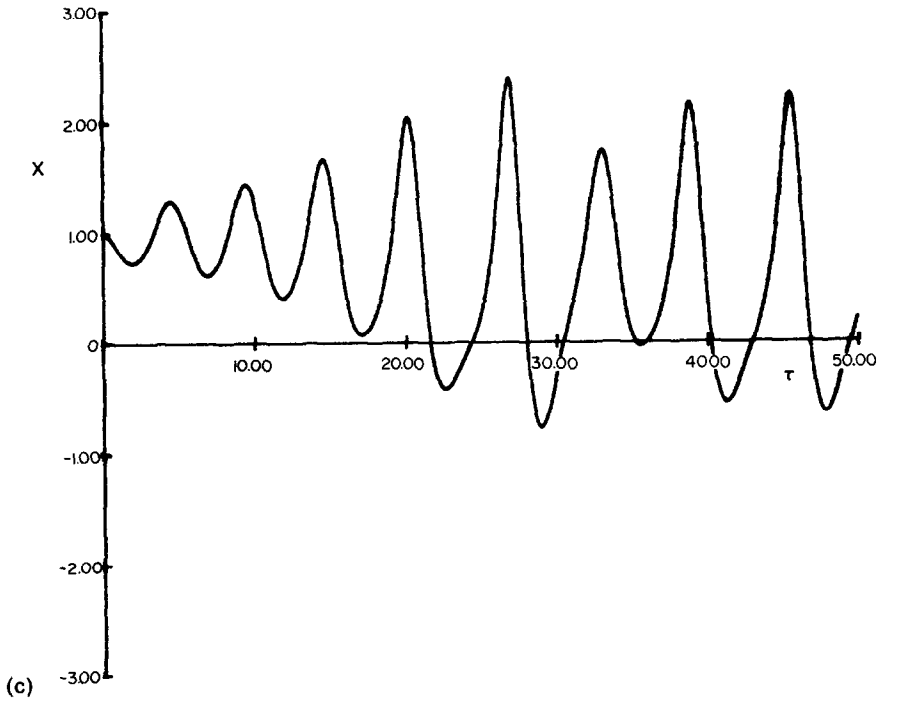

FIG. 6. Numerical solution for $a = 0.5, b = 1$. Initial conditions (1, 1, 1). (a) xy projection, (b) xz projection, and (c) $x(\tau)$.

solutions may appear. The principal difficulty presented by this heating mode is that the origin is always a critical point. This zero velocity is not a valid time-independent solution in experimental models with symmetric heating mode (a). Results shown by Damerell and Schoenhals [7] which purport to demonstrate the contrary are incorrect since they are based on an approximation which is invalidated at small velocities. An exact analysis shows that only two symmetrically placed time-independent solutions exist,

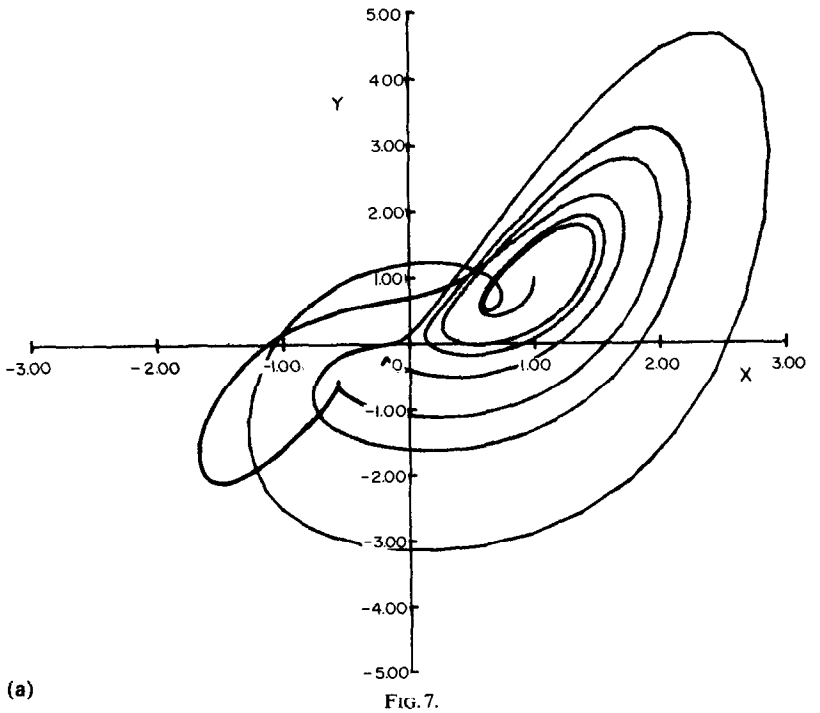

FIG. 7.

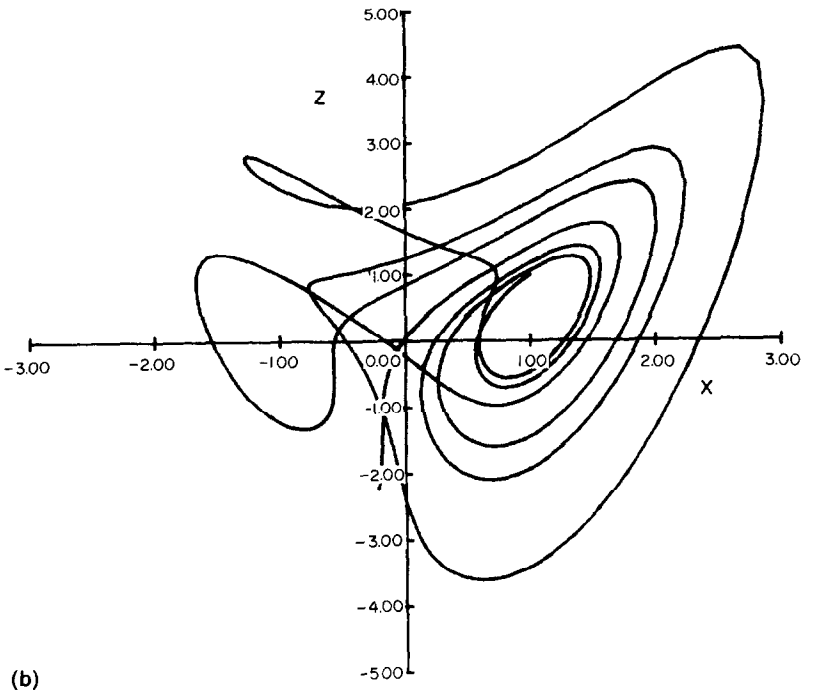

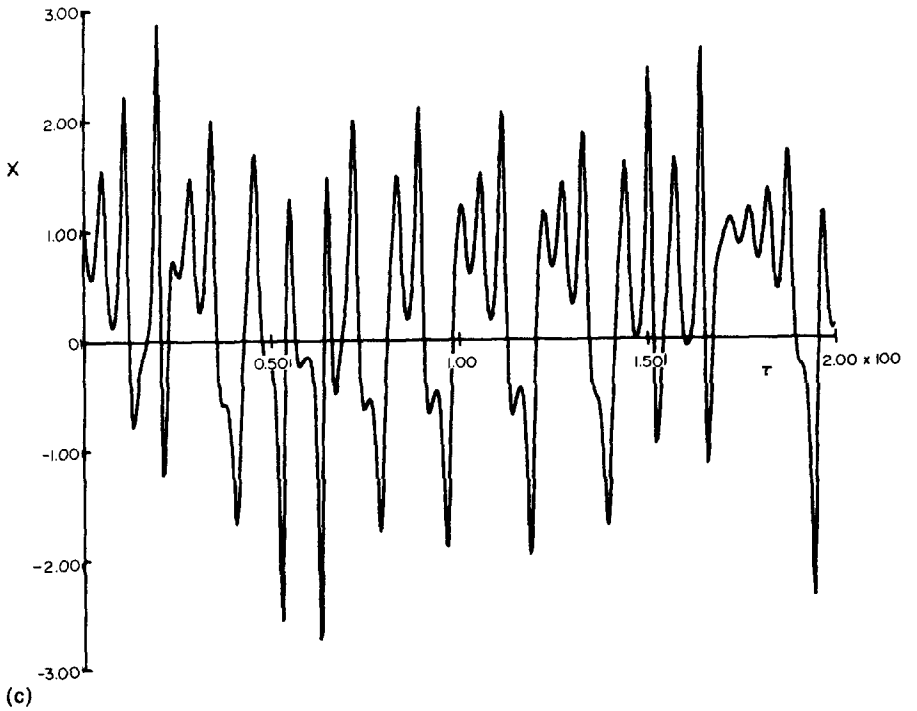

FIG. 7. Numerical solution for $a = 0.25, b = 1$. Initial conditions (1, 1, 1). (a) xy projection, (b) xz projection, and (c) $x(\tau)$.

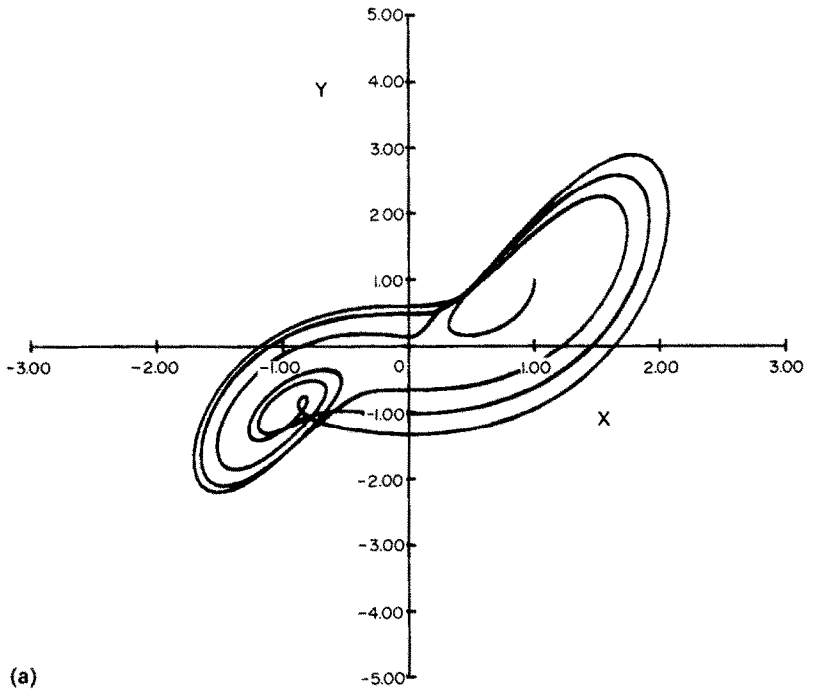
5.00
4.00
Y
3.00
2.00
1.00
-3.00
-2.00
-1.00
0
1.00
2.00
3.00
-1.00
X
-2.00
-3.00
-4.00
-5.00

(a)

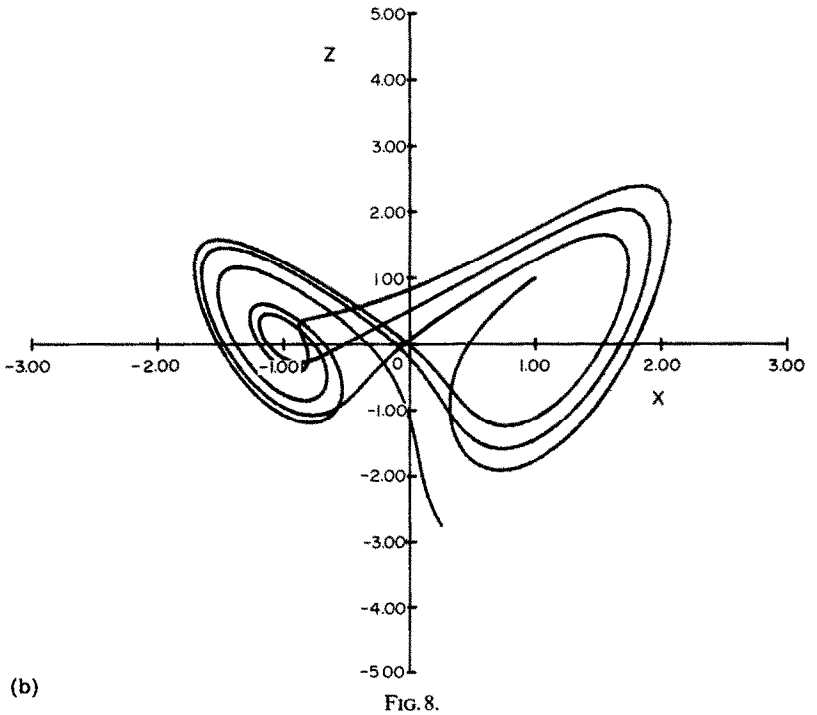
5.00
Z
4.00
3.00
2.00
1.00
-3.00
-2.00
-1.00
0
1.00
2.00
3.00
X
-1.00
-2.00
-3.00
-4.00
-5.00

(b)

FIG. 8.

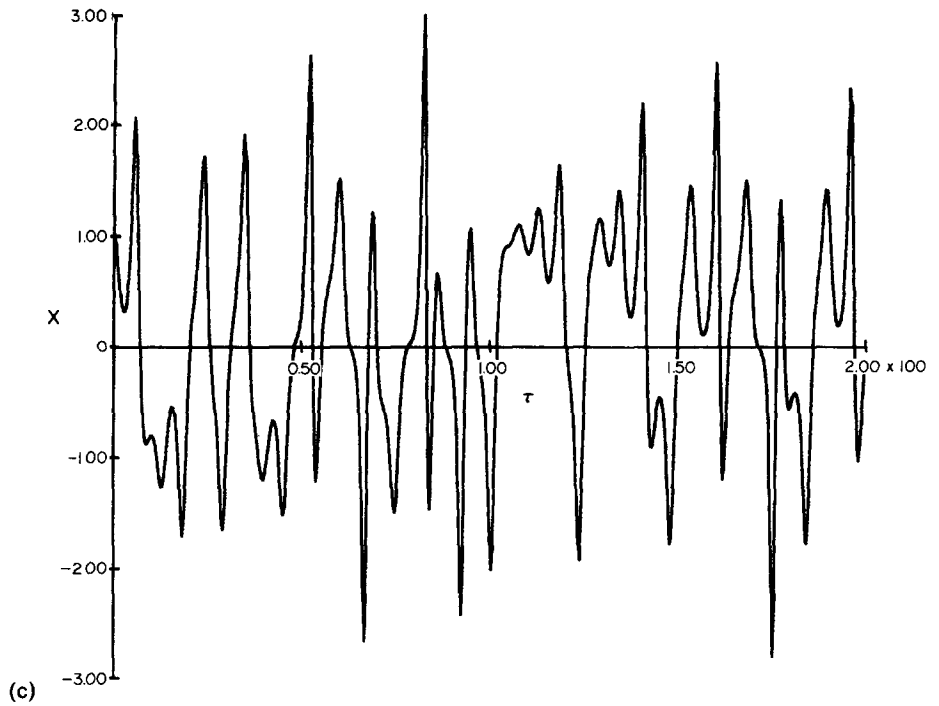

FIG. 8. Numerical solution for $a = 0$, $b = 1$. Initial conditions (1, 1, 1). (a) xy projection, (b) xz projection, and (c) $x(\tau)$.

Table 1. Values of $x'/\bar{x}$ for $a = 0$ and different values of b

b	$x'/\bar{x}$
0.5	0.9943
1.0	0.9914
1.5	0.9970
2.0	1.0007
2.5	0.9948
3.0	0.9963
3.5	0.9976
4.0	0.9997
4.5	0.9968
5.0	0.9962

Initial values of (x, y, z) are (1, 1, 1) and integration is from $\tau = 0$ to 1000.

which is also true for the heating mode (b) analyzed here. In this respect, heating mode (b) is a more realistic approximation to experiments as compared to mode (c). The equations corresponding to heating mode (a) cannot, in general, be reduced to a set of three ordinary differential equations. The infinite set remains coupled.

Acknowledgement—This work was partially funded by the Fondo de Estudios e Investigaciones Ricardo J. Zevada.

REFERENCES

1. M. Sen and C. Treviño, Dynamic analysis of a one-dimensional thermosyphon model, *J. Therm. Engng* **3**, 15–20 (1982).
2. M. Sen and C. Treviño, One dimensional thermosyphon analysis, *Latin Am. J. Heat Mass Transfer* **7**, 135–150 (1983).
3. J. B. Keller, Periodic oscillations in a model of thermal convection, *J. Fluid Mech.* **26**, 599–606 (1966).
4. P. Welander, On the oscillatory instability of a differentially heated fluid loop, *J. Fluid Mech.* **29**, 17–30 (1967).
5. Y. Zvirin and R. Greif, Transient behavior of natural circulation loops, *Int. J. Heat Mass Transfer* **22**, 499–504 (1979).
6. H. F. Creveling, J. F. de Paz, J. Y. Baladi and R. J. Schoenhals, Stability characteristics of a single-phase free convection loop, *J. Fluid Mech.* **67**, 65–84 (1975).
7. P. S. Damerell and R. J. Schoenhals, Flow in a toroidal thermosyphon with angular displacement of heated and cooled sections, *J. Heat Transfer* **101**, 672–675 (1979).
8. R. Greif, Y. Zvirin and A. Mertol, The transient and stability behavior of a natural circulation loop, *J. Heat Transfer* **101**, 684–688 (1979).
9. S. Kaizerman, E. Wacholder and E. Elias, Stability and transient behavior of a vertical toroidal thermosyphon, *ASME Paper*, No. 81-WA/HT-11 (1981).
10. E. Wacholder, S. Kaizerman and E. Elias, Numerical analysis of the stability and transient behavior of natural convection loops, *Int. J. Engng Sci.* **20**, 1235–1254 (1982).
11. A. Mertol and R. Greif, Study of a thermosyphon with a counter-flow heat exchanger, *Proc. VII Int. Heat Transfer Conf.*, Munich, FRG **2**, 239–244 (1982).
12. W. L. Siegmann and L. A. Rubenfeld, A nonlinear model for double-diffusive convection, *SIAM J. appl. Math.* **29**, 540–557 (1975).
13. J. A. Yorke and G. D. Yorke, Chaotic behavior and fluid dynamics. In *Hydrodynamic Instabilities and the Transition to Turbulence* (edited by H. L. Swinney and J. P. Gollub). Springer-Verlag, Berlin (1981).
14. Y. Zvirin, The effect of dissipation on free convection loops, *Int. J. Heat Mass Transfer* **22**, 1539–1546 (1979).
15. A. Mertol, R. Greif and A. T. Giz, The transient, steady

state and stability behavior of a toroidal thermosyphon with parallel-flow heat exchanger, *J. Solar Energy Engng* **105,** 58–65 (1983).
16. H. Stommel and C. Rooth, On the interaction of gravitational and dynamic forcing in simple circulation models, *Deep-Sea Res.* **15,** 165–170 (1968).
17. B. Saltzman, Finite amplitude free convection as an initial value problem, *J. Atmos. Sci.* **19,** 329–341 (1962).
18. E. N. Lorenz, Deterministic nonperiodic flow, *J. Atmos. Sci.* **20,** 130–141 (1963).
19. W. V. R. Malkus, Non-periodic convection at high and low Prandtl number, *Mémoires Société Royale des Science de Liège*, 6e Série, Vol. IV, pp. 125–128 (1972).
20. J. E. Hart, A new analysis of a closed loop thermosyphon, *Int. J. Heat Mass Transfer* **27,** 125–136 (1984).
21. E. Ramos, M. Sen and C. Treviño, Chaotic behavior in convective flows, *Proc. Segunda Escuela Mexicana de Física Estadística* (edited by R. Peralta-Fabi and F. Ramos-Gómez). Soc. Mex. Fis. (In press).
22. M. Sen and C. Treviño, The effect of longitudinal conduction on a solar thermosyphon, *Proc. VIth Mtg Nat. Assoc. Solar Energy*, La Paz, México, pp. 87–90 (In Spanish) (1982).
23. R. K. Miller and A. N. Michel, *Ordinary Differential Equations.* Academic Press, New York (1982).
24. E. Ott, Strange attractors and chaotic motions of dynamical systems, *Rev. Mod. Phys.* **53,** 655–671 (1981).

APPENDIX

Here we transform the toroidal thermosyphon problem with heating flux (a) to a set of ordinary differential equations. For convenience we shall refer to a problem studied by numerous authors [6–8] in which the lower half of the torus is heated by a constant heat flux and the upper half cooled by a heat exchanger with constant wall temperature. Using the notation of Greif *et al.* [8] we have

$$\frac{dw}{d\tau}+\Gamma w=\frac{\pi\Gamma}{4D}\int_0^{2\pi}\phi\cos\theta\,d\theta \tag{A1}$$

$$\frac{\partial\phi}{\partial\tau}+2\pi w\frac{\partial\phi}{\partial\theta}=\begin{cases}-2D\phi, & 0<\theta<\pi\\ 2D, & \pi<\theta<2\pi\end{cases} \tag{A2}$$

where w, ϕ and τ are the non-dimensional velocity, temperature and time, respectively. Γ and D are system parameters. The angle θ is measured as in Fig. 1.

Taking

$$\phi(\theta,\tau)=\sum_{n=0}^{\infty}[C_n(\tau)\cos n\theta+S_n(\tau)\sin n\theta] \tag{A3}$$

from equation (A1) we get

$$\frac{dw}{d\tau}+\Gamma w=\frac{\pi^2\Gamma}{4D}C_1(\tau).$$

Equation (A2) gives, for the two modes,

$$\frac{dC_m}{d\tau}+2\pi wmS_m=-DC_m+\frac{D}{\pi}\sum_{\substack{n=0\\ n\neq m}}^{\infty}S_n[(-1)^{m+n}-1]\frac{2n}{n^2-m^2}$$

$$\frac{dS_m}{d\tau}-2\pi wmC_m=-DS_m+\frac{D}{\pi}\sum_{\substack{n=0\\ n\neq m}}^{\infty}C_n[(-1)^{n+m}-1]\frac{2m}{m^2-n^2}+\frac{2D}{\pi m}[1-(-1)^m].$$

These constitute an infinite set of coupled equations. If the summation in (A3) is taken only over odd values of n, as in [20], the first three equations decouple from the rest and can be transformed to the Lorenz equations through a simple change in variables.

LE THERMOSIPHON AVEC FLUX THERMIQUE CONNU

Résumé—On discute le comportement d'un thermosiphon avec un flux de chaleur connu autour de la boucle. Des critères sont établis pour les solutions permanentes. Les équations du problème variable sont transformées en un système infini d'équations différentielles. La vitesse peut néanmoins être déterminée à partir d'un système de trois équations qui est découplé du reste. L'existence et la stabilité des points critiques de ces équations sont examinées, et des solutions numériques typiques pour différentes valeurs des paramètres opératoires sont présentées. Des solutions chaotiques sont montrées possibles.

DER TORUSFÖRMIGE THERMOSYPHON MIT VORGEGEBENER WÄRMESTROMDICHTE

Zusammenfassung—Dieser Aufsatz behandelt das Verhalten eines torusförmigen Thermosyphons mit am gesamten Umfang vorgegebener Wärmestromdichte. Zuerst werden die Kriterien für stationäre Lösungen festgelegt. Dann werden die Gleichungen, die das instationäre Verhalten beschreiben, in einen unendlich großen Satz von gewöhnlichen Differentialgleichungen transformiert. Die Strömungsgeschwindigkeit läßt sich dabei allerdings aus einem Satz von drei Gleichungen ermitteln, die nicht mit den restlichen gekoppelt sind. Existenz und Stabilität der kritischen Punkte dieser Gleichungen werden überprüft. Für verschiedene Werte der wesentlichen Parameter werden typische numerische Lösungen angegeben. Dabei zeigt sich, daß chaotische Lösungen möglich sind.

ТЕРМОСИФОН ТОРОИДАЛЬНОЙ ФОРМЫ С ИЗВЕСТНОЙ ПЛОТНОСТЬЮ ТЕПЛОВОГО ПОТОКА

Аннотация—Рассматривается режим работы термосифона тороидальной формы с известной плотностью теплового потока по контуру. Вначале выведены критерии стационарных решений. Затем основные нестационарные уравнения преобразованы в бесконечную систему обычных дифференциальуравнений. Однако показано, что скорость потока может быть определена из системы, состоящей только из трех уравнений. Рассматривается существование и устойчивость критических точек этих уравнений, и представлены типичные численные решения для различных значений основных параметров. Показана возможность появления хаотических решений.